

Chiroptical and Lectin Recognition Properties of Glycoconjugated Poly(phenylacetylene)s Featuring Variable Saccharide Functionalities

Issei Otsuka,[†] Takayoshi Hongo,[†] Hiroshi Nakade,[†] Atsushi Narumi,[†] Ryosuke Sakai,[†] Toshifumi Satoh,[†] Harumi Kaga,[‡] and Toyoji Kakuchi*,[†]

Division of Biotechnology and Macromolecular Chemistry, Graduate School of Engineering, Hokkaido University, Sapporo, 060-8628, Japan, and National Institute of Advanced Industrial Science and Technology (AIST), Sapporo, 062-8517, Japan

Received September 15, 2007; Revised Manuscript Received October 8, 2007

ABSTRACT: We report the chiroptical properties and lectin affinities of poly(phenylacetylene)s featuring saccharide functionalities including D-glucopyranoside and D-galactopyranoside. The glycoconjugated poly(phenylacetylene)s were synthesized by rhodium mediated polymerization from phenylacetylene monomers containing a series of saccharide groups; 4-ethynylphenyl 2,3,4,6-tetra-O-acetyl- α -D-glucopyranoside (**PA- α -Glc-OAc**), β -D-glucopyranoside (**PA- β -Glc-OAc**), α -D-galactopyranoside (**PA- α -Gal-OAc**), and β -D-galactopyranoside (**PA- β -Gal-OAc**). On the basis of CD and UV–vis experiments, these polymers were found to have biased helical conformations in a variety of solvents, such as CHCl₃, THF, and HFIP. The deprotection of the acetyl groups using CH₃ONa provided the linear saccharide arrays with diverse saccharide functionalities; **poly-PA- α -Glc**, **poly-PA- β -Glc**, **poly-PA- α -Gal**, and **poly-PA- β -Gal**. CD experiments revealed that **poly-PA- α -Glc** and **poly-PA- β -Glc** have identical helical structures, and **poly-PA- α -Gal** and **poly-PA- β -Gal** feature mirror-imaged helical structures. The binding affinities to lectins were demonstrated by a fluorometric assay using the fluorescein isothiocyanate labeled lectins, such as Concanavalin A (FITC-Con A) and peanut agglutinin (FITC-PNA). As expected, increasingly enhanced affinities for Con A and PNA were observed for the helical saccharide arrays in comparison to the monomeric models. Accordingly, the enhanced affinities are essentially correlated with the multivalency and conformational organization of the saccharide functionalities in the arrays.

Introduction

Glycoconjugated macromolecules consisting of multivalent saccharide arrays provide routes to a wide variety of materials for HIV drugs, drug delivery, cell cultures, and biosensors.¹ Branching saccharide arrays can be synthetically produced by the creation of dendritic and hyperbranched macromolecules. For example, Roy et al. reported the preparation of saccharide-carrying multibranching glycopolymers by a solid-phase synthesis using the 2-thiosialic acid derivative and branched L-lysine core structures.² Aoi et al. reported the preparation of fully sugar-substituted dendrimers, i.e., “sugar balls”, through modification of the poly(amidoamine) dendrimer surface with saccharides,³ Stoddart et al. reported the preparation of carbohydrate-containing dendrimers by a convergent synthetic approach,⁴ and we reported the preparation of hyperbranched carbohydrate polymers through the ring-opening multibranching polymerization of anhydro saccharides as cyclic monomers.⁵ Linear saccharide arrays has been reported by Kobayashi et al. for poly(styrene)s,⁶ poly(acrylamide)s,⁷ poly(phenylacetylene)s,⁸ and poly(phenylisocyanide)s⁹ that examined the effects of polymer chains on host–guest affinity. The development of increasingly sophisticated saccharide arrays will be highlighted by the design of saccharide arrays featuring a recognition specificity arising from the three-dimensional organization of the saccharide groups.

To impart the arrays with a three-dimensional registration of saccharides, poly(phenylacetylene)s provide an ideal platform due to their inherent characteristics such as backbone-chirality,

flexible polymer backbones, and π -conjugated properties. Poly(phenylacetylene)s feature one-handed helical conformations determined by the local stereocenters of the side-chain groups. The translation of chiral information makes it possible to coax saccharide groups along the π -conjugated backbones, providing a three-dimensional organization of the saccharide groups within the biased helical conformation. Given the backbone flexibility and π -conjugation properties, poly(phenylacetylene)s exhibit colorimetric and chiroptical changes in response to various external stimuli, providing opportunities for the visualization of guest molecules and differences in the local environments. Thus, modulation of the poly(phenylacetylene)s with variable saccharide groups provides an exquisite approach for creating not only well-defined helical saccharide arrays with a recognition specificity but also pragmatic optical sensors.

Herein, we demonstrate (1) the synthesis of glycoconjugated poly(phenylacetylene)s with α -D-glucopyranoside (**poly-PA- α -Glc**), β -D-glucopyranoside (**poly-PA- β -Glc**), α -D-galactopyranoside (**poly-PA- α -Gal**), and β -D-galactopyranoside (**poly-PA- β -Gal**) using a rhodium catalyst (Scheme 1), (2) the chiroptical properties of the glycoconjugated poly(phenylacetylene)s reflecting solvent-induced conformational fluctuations in the saccharide groups, and (3) a preliminary insight into the lectin recognition affinity of the glycoconjugated poly(phenylacetylene)s.

Experimental Section

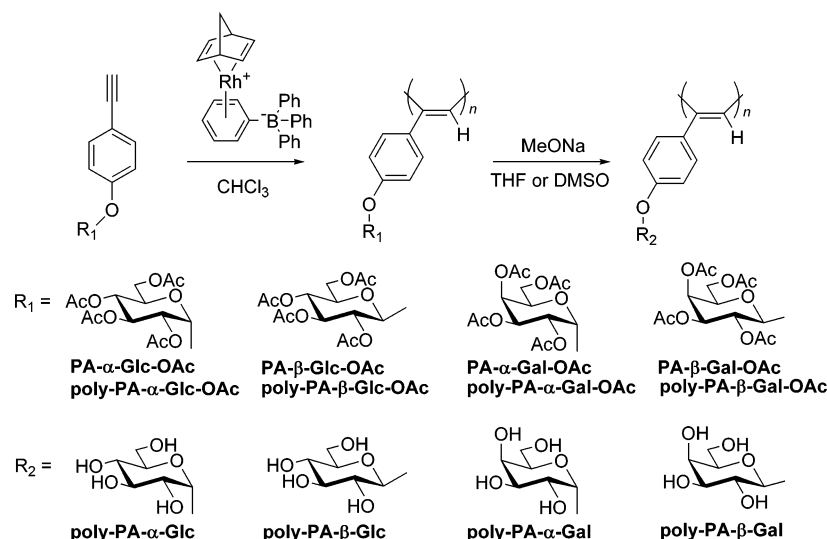
Instruments. The ¹H NMR and ¹³C NMR spectra were recorded using JEOL JNM-EX270 and JEOL JNM-A400II instruments. The size exclusion chromatography equipped with a refractive index detector (Wyatt Technology Optilab rEX), light scattering detector (Wyatt Technology DOWN HELEOS), and viscometer (Wyatt Technology Viscoster). SEC-multiangle laser light scattering (MALLS) was performed at 40 °C in CHCl₃ using two Shodex

* Corresponding author. Phone and fax: +81-11-706-6602. E-mail: kakuchi@poly-bm.eng.hokudai.ac.jp.

[†] Hokkaido University.

[‡] National Institute of Advanced Industrial Science and Technology.

Scheme 1



K-805L columns. IR spectra were recorded using a Perkin-Elmer Paragon 1000 FT-IR spectrometer. The fluorescence spectra were measured in a 10 mm path length using a Jasco FP-6300 spectrofluorometer. The circular dichroism (CD) and ultraviolet–visible (UV–vis) spectra were measured in a 1 mm path length using a Jasco J-720 spectropolarimeter. The optical rotations were measured with a Jasco DIP-1000 digital polarimeter. Preparation of the polymerization solution was carried out in an MBRAUN stainless steel glovebox equipped with a gas purification system (molecular sieves and copper catalyst) under a dry argon atmosphere (H_2O , $O_2 < 1$ ppm). The moisture and oxygen contents in the glovebox were monitored by an MB-MO-SE 1 and an MB-OX-SE 1, respectively.

Materials. $Rh^+(2,5\text{-orborene})[(\eta^6\text{-C}_6\text{H}_5)_3\text{B}^-(\text{C}_6\text{H}_5)_3]$ ($Rh(\text{nbdb})\text{PPh}_4$),¹⁰ 4-ethynylphenyl 2,3,4,6-tetra-*O*-acetyl- β -D-glucopyranoside (**PA- β -Glc-OAc**),¹¹ 4-ethynylphenyl 2,3,4,6-tetra-*O*-acetyl- α -D-galactopyranoside (**PA- α -Gal-OAc**),¹¹ 2,3,4,6-tetra-*O*-acetyl- α -D-glucopyranosyl trichloroacetimidate,¹² and 4-(trimethylsilyl)ethynylphenol¹³ were synthesized by previously reported methods. Tin(IV) chloride (SnCl_4), anhydrous (purity >98%), was purchased from Kanto Chemical Co., Inc. (Tokyo, Japan) and used without further purification. (Trimethylsilyl)acetylene was kindly supplied from Shinetsu Chemical Co., Ltd. (Tokyo, Japan) and used without further purification. Boron trifluoride diethyletherate ($\text{BF}_3 \cdot \text{OEt}_2$) (purity 95%) was purchased from Kanto Chemical Co., Inc. and used after distillation under reduced pressure. Bis(triphenylphosphine)paradium(II) dichloride (purity 99.99%) was purchased from the Sigma-Aldrich Co. (Missouri) and used as received. Tetrabutylammonium fluoride, a 1.0 M solution in tetrahydrofuran, was purchased from the Sigma-Aldrich Co. and used as received. 4-Iodophenol was kindly supplied from Manac, Inc. (Hiroshima, Japan) and used without further purification. Triphenylphosphine (purity >98%) was purchased from Kanto Chemical Co., Inc. and used after being recrystallized from dichloromethane/diethyl ether. The phosphate buffered saline solution (PBS) (0.01 mol L^{-1} , pH 7.4) was purchased from Kanto Chemical Co., Inc. and used as received. The fluorescein isothiocyanate labeled Concanavalin A (FITC-Con A) was purchased from Seikagaku Corp. (Tokyo, Japan) and used without further purification. The fluorescein isothiocyanate labeled peanut agglutinin (FITC-PNA) was purchased from the Sigma-Aldrich Co. and used without further purification.

4-Iodophenyl 2,3,4,6-Tetra-*O*-acetyl- α -D-glucopyranoside. To a stirred mixture of penta-*O*-acetyl- β -D-glucopyranose (24.0 g, 61.5 mmol), 4-iodophenol (19.0 g, 86.4 mmol), and molecular sieves 4 Å in dry CHCl_3 (120 mL) was added SnCl_4 (21.6 mL, 185 mmol), and the reaction mixture was kept at 62–64 °C for 7 h. The mixture was poured into ice-cold aqueous NaHCO_3 (1200 mL) and diluted with CHCl_3 (1200 mL). The solution was filtered through Celite 545, and the residue was washed with CHCl_3 . The organic phase

was rapidly washed with ice–water (800 mL), dried over Na_2SO_4 , and evaporated. The obtained crude product was purified by column chromatography (silica gel, hexane/ethyl acetate, 7:4) to give 4-iodophenyl 2,3,4,6-tetra-*O*-acetyl- α -D-glucopyranoside as a white powder. Yield: 13.6 g (40%). ^1H NMR (CDCl_3): δ 7.60, 6.87 (d, $J = 8.8$ Hz, 4H, aromatic), 5.73–5.63 (m, 2H, H-1, H-2), 5.15 (t, $J = 9.9$ Hz, 1H, H-4), 5.03 (dd, $J = 3.5, 10.3$ Hz, 1H, H-3), 4.24 (dd, $J = 4.7, 12.5$ Hz, 1H, H-6), 4.11–4.02 (m, 2H, H-5, H-6), 2.06, 2.05, 2.05, 2.04 (s, 12H, acetyl). ^{13}C NMR (CDCl_3): δ 170.49, 170.13, 170.11, 169.55 (4C, CO), 155.87, 138.54, 118.81, 85.79 (6C, aromatic), 94.18 (1C, C-1), 70.32, 69.89, 68.18, 68.16, 61.50 (5C, C-2, C-3, C-4, C-5, C-6), 20.69, 20.65, 20.61, 20.58 (4C, CH_3). Anal. Calcd for $\text{C}_{20}\text{H}_{23}\text{IO}_{10}$: C, 43.65; H, 4.21; I, 23.06. Found: C, 43.46; H, 4.14; I, 23.36.

4-Ethynylphenyl 2,3,4,6-Tetra-*O*-acetyl- α -D-glucopyranoside (PA- α -Glc-OAc). To a stirred solution of 4-iodophenyl 2,3,4,6-tetra-*O*-acetyl- α -D-glucopyranoside (13.5 g, 24.5 mmol), $(\text{Ph}_3\text{P})_2\text{PdCl}_2$ (340 mg, 0.49 mmol), CuI (190 mg, 1.00 mmol), and triethylamine (84.0 mL) in dry THF (100 mL) was added (trimethylsilyl)acetylene (4.20 mL, 30.0 mmol) at room temperature under a nitrogen atmosphere. After stirring for 15 h, the reaction mixture was diluted with CHCl_3 (300 mL) and filtered. The filtrate was washed with H_2O and dried over Na_2SO_4 . The solvent was evaporated, and the crude product was stirred with tetrabutylammonium fluoride (15.0 mL; 1.00 mol L^{-1} in THF) in dry CH_2Cl_2 for 30 min at room temperature under a nitrogen atmosphere. The reaction mixture was washed with H_2O and dried over Na_2SO_4 . After evaporating the solvent, the crude product was purified by column chromatography (silica gel, CH_2Cl_2 /ethyl acetate, 10:1) and recrystallized from hexane with a few drops of methanol to give **PA- α -Glc-OAc** as a white solid. Yield: 8.47 g (77%). ^1H NMR (CDCl_3): δ 7.44, 7.05 (d, $J = 8.8$ Hz, 4H, aromatic), 5.75 (d, $J = 3.4$ Hz, 1H, H-1), 5.69 (t, $J = 9.8$ Hz, 1H, H-2), 5.15 (t, $J = 9.9$ Hz, 1H, H-4), 5.05 (dd, $J = 3.9, 10.3$ Hz, 1H, H-3), 4.24 (dd, $J = 4.6, 12.5$ Hz, 1H, H-6), 4.12–4.02 (m, 2H, H-5, H-6), 3.05 (s, 1H, $\text{C}\equiv\text{C}-\text{H}$), 2.07, 2.06, 2.04, 2.03 (s, 12H, acetyl). ^{13}C NMR (CDCl_3): δ 170.39, 170.03, 169.46 (4C, CO), 156.19, 133.58, 116.70, 116.42 (6C, aromatic), 93.95 (1C, C-1), 82.91 (1C, $-\text{Ar}-\text{C}\equiv\text{C}-\text{H}$), 76.65 (1C, $-\text{Ar}-\text{C}\equiv\text{C}-\text{H}$), 70.21, 69.85, 68.13, 68.11, 61.43 (5C, C-2, C-3, C-4, C-5, C-6), 20.61, 20.55, 20.53, 20.49 (4C, CH_3). $[\alpha]_D^{25} = +240.4^\circ$ (c 1.0, CHCl_3). Anal. Calcd for $\text{C}_{22}\text{H}_{24}\text{O}_{10}$: C, 58.93; H, 5.39. Found: C, 58.97; H, 5.38.

4-Ethynylphenyl 2,3,4,6-Tetra-*O*-acetyl- β -D-galactopyranoside (PA- β -Gal-OAc). A mixture of 2,3,4,6-tetra-*O*-acetyl- α -D-glucopyranosyl trichloroacetimidate (2.22 g, 4.51 mmol), 4-(trimethylsilyl)ethynylphenol (1.40 g, 7.34 mmol), and molecular sieves 4 Å in dry CH_2Cl_2 (50 mL) was stirred at -25°C for 30 min under a nitrogen atmosphere. To the mixture was slowly added $\text{BF}_3 \cdot \text{OEt}_2$

(0.59 mL, 4.88 mmol) with stirring for 30 min, and the reaction was quenched with pyridine (1.80 mL). After evaporating the solvent, the mixture was purified by flash column chromatography (silica gel, hexane/ethyl acetate, 2:1). The obtained product was stirred with tetrabutylammonium fluoride (1.50 mL; 1.00 mol L⁻¹ in THF) in dry CH₂Cl₂ (90 mL) for 30 min. To the mixture was added aqueous NH₄Cl (100 mL) and extracted with CHCl₃. The organic phase was dried over Na₂SO₄ and then evaporated. The obtained crude product was purified by column chromatography (silica gel, hexane/ethyl acetate, 4:3) and recrystallized from diethyl ether to give **PA-β-Gal-OAc** as a white solid. Yield: 1.74 g (86%). ¹H NMR (CDCl₃): δ 7.43, 6.95 (d, *J* = 8.9 Hz, 4H, aromatic), 5.54–5.44 (m, 2H, H-2, H-4), 5.11 (dd, *J* = 3.5, 10.4 Hz, 1H, H-3), 5.06 (d, *J* = 7.9 Hz, 1H, H-1), 4.22–4.07 (m, 3H, H-5, H-6), 3.03 (s, 1H, C≡C–H), 2.19, 2.07, 2.02 (s, 12H, acetyl). ¹³C NMR (CDCl₃): δ 170.29, 170.17, 170.05, 169.29 (4C, CO), 156.97, 133.57, 116.97, 116.70 (6C, aromatic), 99.18 (1C, C1), 82.97 (1C, –Ar–C≡C–H), 76.66 (1C, –Ar–C≡C–H), 71.12, 70.72, 68.50, 66.79, 61.33 (5C, C-2, C-3, C-4, C-5, C-6), 20.66, 20.60, 20.52 (4C, CH₃). [α]_D²³ = +12.3° (c 1.0, CHCl₃). Anal. Calcd for C₂₂H₂₄O₁₀: C, 58.93; H, 5.39. Found: C, 58.64; H, 5.40.

Poly(4-ethynylphenyl 2,3,4,6-Tetra-O-acetyl-α-D-glucopyranoside) (poly-PA-α-Glc-OAc). A typical polymerization method is as follows (Method A): to a stirred solution of **PA-α-Glc-OAc** (1.00 g, 2.23 mmol) in dry CHCl₃ (15 mL) was added a solution of Rh(norbornadiene)BPh₄ (23 mg, 45 μmol) in dry CHCl₃ (7 mL) under an argon atmosphere. After 20 h, the reaction was terminated by adding triphenylphosphine (70 mg, 0.27 mmol) and then poured into a large amount of methanol. The precipitate was filtered off and dried in vacuo to give **poly-PA-α-Glc-OAc** as a yellow powder. Yield: 89%. *M*_{w,SEC-MALLS} (in CHCl₃): 2.49 × 10⁵. *M*_w/*M*_n: 1.46. ¹H NMR (CDCl₃): δ 7.79–6.28 (br, aromatic), 6.20–4.59 (br, =CH and saccharide moiety), 2.60–1.40 (br, acetyl). IR (KBr, cm⁻¹) 1756 (ν_{C=O}). [α]_D²³ = +296.3° (c 1.0, CH₂Cl₂).

Poly(4-ethynylphenyl 2,3,4,6-Tetra-O-acetyl-β-D-glucopyranoside) (poly-PA-β-Glc-OAc). Method A was applied to **PA-β-Glc-OAc** (1.00 g, 2.23 mmol) and Rh(norbornadiene)BPh₄ (23 mg, 45 μmol) in dry CHCl₃ (22 mL). Yield: 83%. *M*_{w,SEC-MALLS} (in CHCl₃): 1.43 × 10⁶. *M*_w/*M*_n: 1.57. ¹H NMR (CDCl₃): δ 7.40–6.70 (br, aromatic), 6.00–4.65 (br, =CH and saccharide moiety), 4.60–3.63 (br, saccharide moiety), 2.60–1.40 (br, acetyl). IR (KBr, cm⁻¹) 1756 (ν_{C=O}). [α]_D²³ = +70.9° (c 1.0, DMSO).

Poly(4-ethynylphenyl 2,3,4,6-Tetra-O-acetyl-α-D-galactopyranoside) (poly-PA-α-Gal-OAc). Method A was applied to **PA-α-Gal-OAc** (1.00 g, 2.23 mmol) and Rh(norbornadiene)BPh₄ (23 mg, 45 μmol) in dry CHCl₃ (22 mL). Yield: 98%. *M*_{w,SEC-MALLS} (in CHCl₃): 7.26 × 10⁵. *M*_w/*M*_n: 1.47. ¹H NMR (CDCl₃): δ 7.50–6.10 (br, aromatic), 6.06–4.73 (br, =CH and saccharide moiety), 4.65–3.18 (br, saccharide moiety), 2.60–1.40 (br, acetyl). IR (KBr, cm⁻¹) 1755 (ν_{C=O}). [α]_D²³ = +380.3° (c 1.0, DMSO).

Poly(4-ethynylphenyl 2,3,4,6-Tetra-O-acetyl-β-D-galactopyranoside) (poly-PA-β-Gal-OAc). Method A was applied to **PA-β-Gal-OAc** (1.00 g, 2.23 mmol) and Rh(norbornadiene)BPh₄ (23 mg, 45 μmol) in dry CHCl₃ (22 mL). Yield: 88%. *M*_{w,SEC-MALLS} (in CHCl₃): 1.74 × 10⁵. *M*_w/*M*_n: 2.05. ¹H NMR (CDCl₃): δ 7.80–4.66 (br, aromatic, =CH, and saccharide moiety), 4.55–3.62 (br, saccharide moiety), 3.00–1.00 (br, acetyl). IR (KBr, cm⁻¹) 1756 (ν_{C=O}). [α]_D²³ = –255.3° (c 1.0, DMSO).

Poly(4-ethynylphenyl-α-D-glucopyranoside) (poly-PA-α-Glc). A typical deacetyl method is as follows (Method B): to a stirred solution of **poly-PA-α-Glc-OAc** (0.30 g) in THF (60 mL) was added NaOCH₃ (1 mL; 1 mol L⁻¹ in MeOH). After 2 h, water (200 mL) was added to dissolve the precipitate. The mixture was dialyzed in a cellulose tube against water for 2 days and then lyophilized to give **poly-PA-α-Glc** as a yellow powder. Yield: approximately 100%. ¹H NMR (DMSO-*d*₆): δ 7.62–6.05 (br, aromatic), 5.45–4.11 (br, =CH and saccharide moiety), 3.88–2.57 (br, OH). IR (KBr, cm⁻¹) 3416 (ν_{O–H}). [α]_D²³ = +457.2° (c 0.5, DMSO).

Poly(4-ethynylphenyl-β-D-glucopyranoside) (poly-PA-β-Glc). Method B was applied to **poly-PA-β-Glc-OAc** (0.30 g) in DMSO (60 mL) and NaOCH₃ (1 mL; 1 mol L⁻¹ in MeOH). Yield: approximately 100%. ¹H NMR (CDCl₃): δ 7.60–5.86 (br, aromatic), 5.58–3.89 (br, =CH and saccharide moiety), 3.43–2.57 (br, OH). IR (KBr, cm⁻¹) 3416 (ν_{O–H}). [α]_D²³ = –353.5° (c 0.5, DMSO).

Poly(4-ethynylphenyl-α-D-galactopyranoside) (poly-PA-α-Gal). Method B was applied to **poly-PA-α-Gal-OAc** (0.30 g) in THF (60 mL) and NaOCH₃ (1 mL; 1 mol L⁻¹ in MeOH). Yield: approximately 100%. ¹H NMR (CDCl₃): δ 7.68–5.96 (br, aromatic), 5.96–4.19 (br, =CH and saccharide moiety), 4.14–2.67 (br, saccharide moiety and OH). IR (KBr, cm⁻¹) 3378 (ν_{O–H}). [α]_D²³ = +500.5° (c 0.5, DMSO).

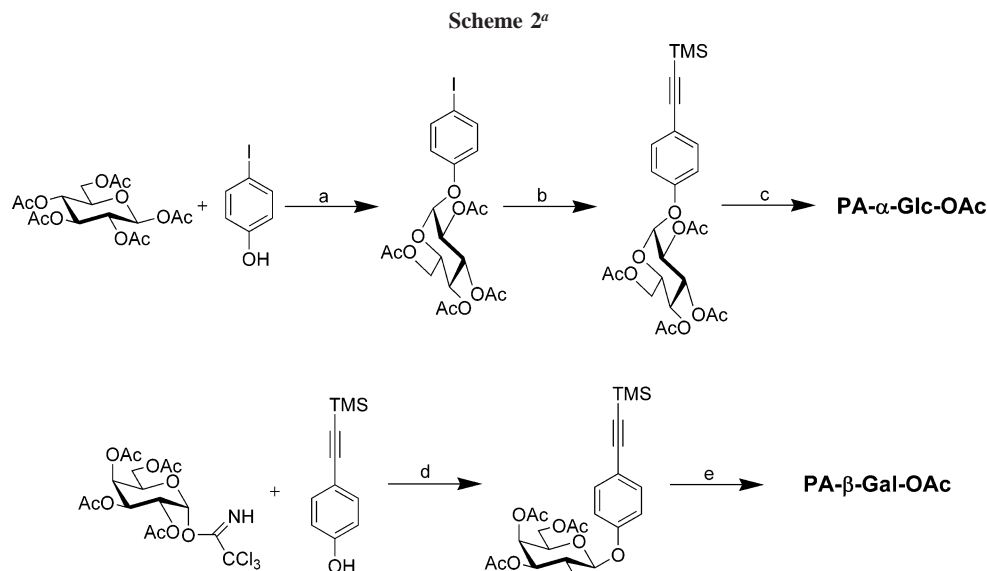
Poly(4-ethynylphenyl-β-D-galactopyranoside) (poly-PA-β-Gal). Method B was applied to **poly-PA-β-Gal-OAc** (0.30 g) in THF (60 mL) and NaOCH₃ (1 mL; 1 mol L⁻¹ in MeOH). Yield: approximately 100%. ¹H NMR (CDCl₃): δ 7.66–5.98 (br, aromatic), 5.37–4.00 (br, =CH and saccharide moiety), 3.93–2.53 (br, saccharide moiety and OH). IR (KBr, cm⁻¹) 3348 (ν_{O–H}). [α]_D²³ = –484.6° (c 0.5, DMSO).

CD and UV–Visible Measurements. The CD and UV–vis spectra were measured in a 1 mm quartz cell at room temperature. The polymer concentration, which was calculated on the basis of the monomeric units, was 3.6 mmol L⁻¹ for **poly-PA-α-Glc**, **poly-PA-β-Glc**, **poly-PA-α-Gal**, and **poly-PA-β-Gal**.

Fluorometric Assay of Lectin-Binding. The fluorescence spectra were measured in a 10 mm quartz cell at 25 °C. A typical procedure is described as follows: aliquots (2 μL) of a stock solution of **poly-PA-α-Glc** (10 mM) in PBS (pH 7.4) were added every 30 min to a solution of FITC-Con A (24 nM, 1.8 mL) in PBS. The fluorescence spectra (500–600 nm) were recorded with excitation at 490 nm. The excitation and emission bandwidth were 5 nm.

Results and Discussion

Synthesis of Poly(phenylacetylene)s with Variable Saccharide Functionalities. To provide poly(phenylacetylene)s with diverse saccharides functionalities, the glycoconjugated phenylacetylenes were prepared through the α- and β- selective glycosylations and the Sonogashira–Hagiwara coupling reaction. 4-Ethynylphenyl 2,3,4,6-tetra-O-acetyl-β-D-glucopyranoside (**PA-β-Glc-OAc**) and α-D-galactopyranoside (**PA-α-Gal-OAc**) were synthesized using previously reported methods.¹¹ The synthesis of the α-D-glucopyranoside (**PA-α-Glc-OAc**) and β-D-galactopyranoside (**PA-β-Gal-OAc**) were carried out using the procedures presented in Scheme 2. These glycoconjugated monomers were then polymerized using Rh(norbornadiene)BPh₄ (Rh(nbd)BPh₄) as a catalyst in dry CHCl₃ at 30 °C for 20 h (Table 1). All the polymerizations homogeneously proceeded to yield dark red viscous products and then purified by reprecipitation with methanol to give the glycoconjugated poly(phenylacetylene)s as yellow powders in high yields (>83%). ¹H NMR spectra of the resultant polymers (**poly-PA-α-Glc-OAc**, **poly-PA-β-Glc-OAc**, **poly-PA-α-Gal-OAc**, and **poly-PA-β-Gal-OAc**) confirmed the structures of the poly(phenylacetylene)s with the saccharide residues. GPC analysis using a refractive index detector, light scattering detector, and viscometer (SEC-MALLS) exhibited unimodal peaks for all the glycoconjugated poly(phenylacetylene)s, resulting in the molecular weights (*M*_w) of 2.49 × 10⁵, 1.43 × 10⁶, 7.26 × 10⁵, and 1.74 × 10⁵ for **poly-PA-α-Glc-OAc**, **poly-PA-β-Glc-OAc**, **poly-PA-α-Gal-OAc**, and **poly-PA-β-Gal-OAc**, respectively (Table 1). Finally, these polymers were hydrolyzed using NaOCH₃ to provide helical arrays consisting of poly(phenylacetylene)s and diverse saccharide functionalities to demonstrate



^a Reagents: (a) SnCl_4 , CHCl_3 , 62–64 °C, (b) trimethylsilyl acetylene, CuI , $(\text{Ph}_3\text{P})_2\text{PdCl}_2$, Et_3N , room temperature (rt), (c) Bu_4NF , CH_2Cl_2 , rt, (d) $\text{BF}_3\cdot\text{OEt}_2$, CH_2Cl_2 , –25 °C, (e) Bu_4NF , CH_2Cl_2 , rt.

Table 1. Polymerization of **PA- α -Glc-OAc**, **PA- β -Glc-OAc**, **PA- α -Gal-OAc**, and **PA- β -Gal-OAc** Using **Rh(nbd)BPh₄**^a

glycoconjugated polymers	yield (%) ^b	$M_w \times 10^{-5}$ ^c	M_w/M_n ^c
poly-PA-α-Glc-OAc	89	2.49	1.46
poly-PA-β-Glc-OAc	83	14.3	1.57
poly-PA-α-Gal-OAc	98	7.26	1.47
poly-PA-β-Gal-OAc	88	1.74	2.05

^a Conditions: [monomer] = 0.1 M.; [monomer]/[Rh(nbd)BPh₄] = 50.; solvent, CHCl_3 ; temp, 30 °C; time, 20 h. ^b Methanol insoluble part.

^c Determined by SEC-MALLS in CHCl_3 .

the affinities toward lectins (**poly-PA- α -Glc**, **poly-PA- β -Glc**, **poly-PA- α -Gal**, and **poly-PA- β -Gal**).

Chiroptical Properties of Glycoconjugated Poly(phenylacetylene)s. The structural conformation of the glycoconjugated poly(phenylacetylene)s was demonstrated on the basis of the circular dichroism (CD) and ultraviolet–visible (UV–vis) spectra. These results provided significant evidence for a variety of one-handed helical structures of the glycoconjugated poly(phenylacetylene)s, showing that the characteristics of the π -conjugated properties and helical structures of the poly(phenylacetylene)s are significantly dependent on the saccharide functionalities. Figure 1 shows the CD and UV–vis spectra of **poly-PA- α -Glc-OAc**, **poly-PA- β -Glc-OAc**, **poly-PA- α -Gal-OAc**, and **poly-PA- β -Gal-OAc** in CH_2Cl_2 at room temperature. **Poly-PA- α -Glc-OAc** induced a first negative Cotton effect at 444 nm, a second positive Cotton effect at 379 nm, a third negative Cotton effect at 340 nm, and a fourth positive Cotton effect at 275 nm. Similar split-type Cotton effects were observed for the other glycoconjugated poly(phenylacetylene)s in the long absorption region of the π -conjugated polyacetylene backbone (250–500 nm). The chiroptical properties of the backbones evidently demonstrate a conformational chirality and thus the one-handed helical conformations of the π -conjugated double bonds in the backbones. The biased helical structures are dictated by the pendant saccharide functionalities, resulting in a variety of CD profiles (Figure 1). **Poly-PA- α -Glc-OAc** prominently showed strong Cotton effects whereas relatively weak signals were observed for **poly-PA- α -Gal-OAc** in CH_2Cl_2 (black and green in Figure 1). This result signifies that the stereocenter at the 4-position in the pyranoside ring is crucial for the configuration–conformation chiral translation from the sugar to phenylacetylene backbones in **poly-PA- α -Glc-OAc** and **poly-**

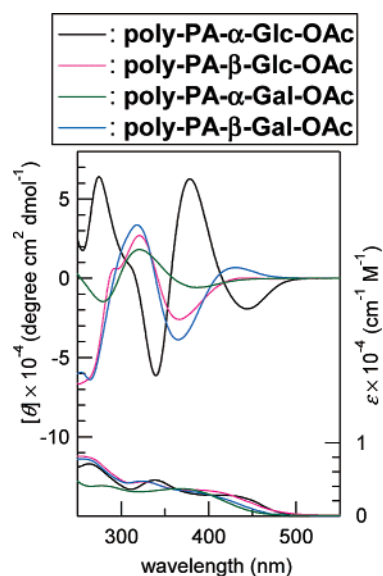


Figure 1. CD (upper) and UV–vis (lower) spectra of (A) **poly-PA- α -Glc** and **poly-PA- β -Glc** and (B) **poly-PA- α -Gal** and **poly-PA- β -Gal** in H_2O at room temperature.

PA- α -Gal-OAc (Figure 1). In clear contrast, **poly-PA- β -Glc-OAc** and **poly-PA- β -Gal-OAc** have essentially identical characteristics of biased helical structures in CH_2Cl_2 ; **poly-PA- β -Glc-OAc** and **poly-PA- β -Gal-OAc** showed almost matching CD profiles (blue and red in Figure 1). The structural difference between the β -Glc and β -Gal groups has no ability to execute the chiral translation in CH_2Cl_2 . These results suggest that the chiral translation from the pendant sugar groups to the polyacetylene backbone is significantly sensitive to the local stereocenters of the sugar functionalities.

As expected, use of variable solvents such as HFIP, chloroform, dichloromethane, DMSO, and THF results in a solvent-induced conformational fluctuation of the pendant sugar functionalities, leading to diverged CD and UV–vis profiles as a consequence of the variety of backbone conformations (Figure 2 and Supporting Information). The remarkable absorptions with the maxima at 470 and 500 nm in the UV–vis profiles were observed with HFIP and CHCl_3 , respectively. The significant solvatochromism promoted substantial visible color changes from

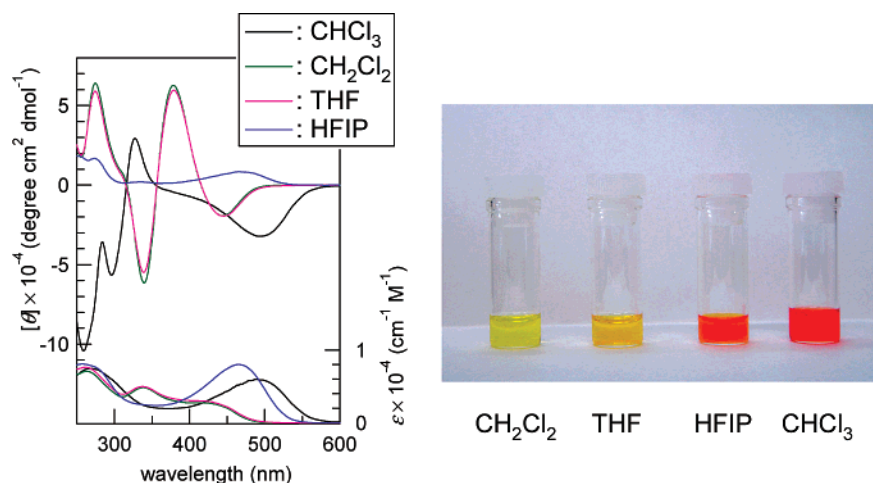


Figure 2. CD (upper) and UV-vis (lower) spectra of **poly-PA-α-Glc-OAc** in THF, CH₂Cl₂, HFIP, and CHCl₃ at room temperature.

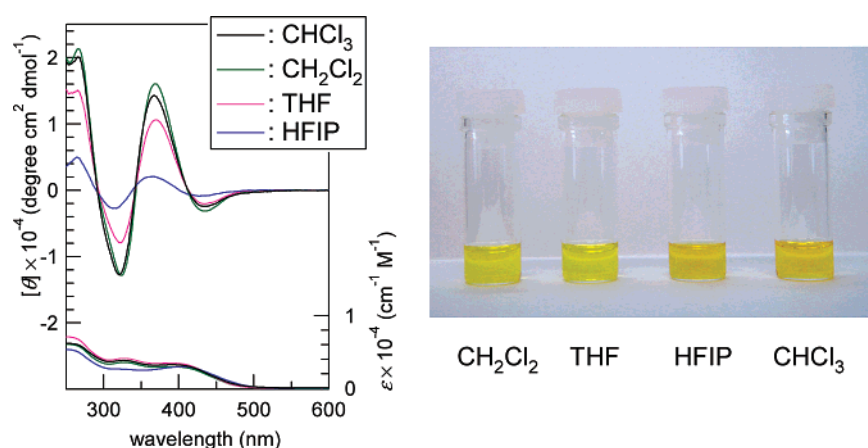


Figure 3. CD (upper) and UV-vis (lower) spectra of **poly(PA_{0.5}-co-PA-α-Glc-OAc_{0.5})** in THF, CH₂Cl₂, HFIP, and CHCl₃ at room temperature.

yellow to red (Figure 2). It was found that no red-shift was observed in CHCl₃ for the β-glycoconjugated poly(phenylacetylene)s, such as **poly-PA-β-Glc-OAc** and **poly-PA-β-Gal-OAc** (see Supporting Information). The pronounced absorptions around 470 nm were accompanied by the corresponding Cotton effects in the CD spectra, and feasibility of the solvatochromism is dependent on the saccharide functionalities. These results suggest that the observed solvatochromism is strongly correlated with the interplay between the poly(phenylacetylene) backbones and saccharide functionalities.

To provide further insight into the solvatochromism, the control, the less-saccharide functionalized copolymer consisting of phenylacetylene and **PA-α-Glc-OAc** (**poly(PA_{0.5}-co-PA-α-Glc-OAc_{0.5})**),¹⁴ was prepared, and the CD and UV-vis spectra were recorded in variable solvents including CH₂Cl₂, THF, HFIP, and CHCl₃ (see Figure 3). The control **poly(PA_{0.5}-co-PA-α-Glc-OAc_{0.5})** showed very consistent CD and UV-vis profiles in a variety of solvents, essentially demonstrating the identical helical structures over the solvent-induced conformational fluctuation of the Glc functionalities. This result clearly revealed that the densely packed saccharide functionalities in **Poly-PA-α-Glc-OAc** make it possible to mediate the solvatochromism as a direct consequence of the helical backbone adaptation. This adaptation is susceptible to the conformational fluctuation of the saccharide functionalities in the various solvents. The control **poly(PA_{0.5}-co-PA-α-Glc-OAc_{0.5})** featuring a chiral translation from the saccharide functionalities to the backbones is, however, incapable of the adaptation due to less-

densely packed saccharide functionalities. The backbone adaptability promoted the adjustment of the twist angle between the π-conjugated double bonds of the backbones, resulting in significant color changes.¹⁵

Figure 4 shows the CD and UV-vis spectra of the acetyl group-free glycoconjugated poly(phenylacetylene)s (**poly-PA-α-Glc**, **poly-PA-β-Glc**, **poly-PA-α-Gal**, and **poly-PA-β-Gal**) in H₂O. The intense Cotton effects in the long absorption region of the backbone (250–500 nm) indicate that these glycoconjugated polymers also feature one-handed helical conformations even in polar solvents, such as H₂O and DMSO (see Supporting Information). The quite consistent CD profiles of **poly-PA-α-Glc** and **poly-PA-β-Glc** in Figure 4A are responsible for the matching helical structures with α-Glc and β-Glc, respectively. Interestingly, **poly-PA-β-Glc** showed mirror-imaged CD profiles in H₂O and DMSO due to the solvent-induced conformational fluctuation of β-Glc, providing evidence for the viability of the backbone adaptation even in polar solvents (see Supporting Information). The CD spectra of **poly-PA-α-Gal** and **poly-PA-β-Gal** exhibited mirror-imaged profiles in H₂O (Figure 4B), indicative of reverse helical structures for **poly-PA-α-Gal** and **poly-PA-β-Gal**. The combination of the chiral translation and backbone adaptability in glycoconjugated poly(phenylacetylene)s permits the three-dimensional organization of saccharides; the α- and β-Glc functionalities are arranged in the same sense of the helical structures, and the α- and β-Gal functionalities are organized in the opposite sense of the helical structures in H₂O.

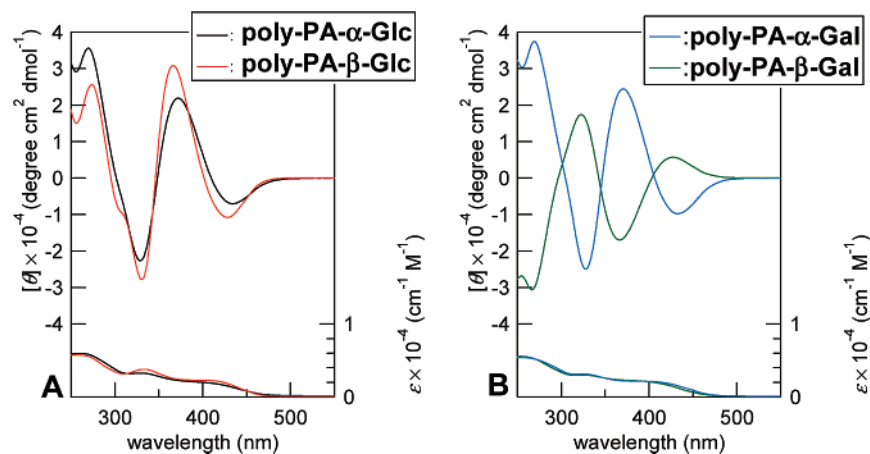


Figure 4. CD (upper) and UV-vis (lower) spectra of (A) **poly-PA-α-Glc** and **poly-PA-β-Glc** and (B) **poly-PA-α-Gal** and **poly-PA-β-Gal** in H₂O at room temperature.

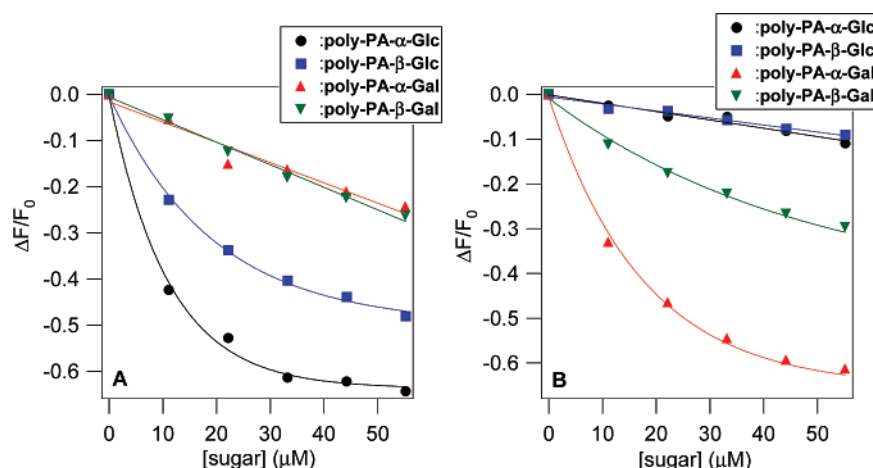


Figure 5. Dependence of fluorescence intensity of FITC-Con A (A) and FITC-PNA (B) at 517 nm (ex = 490 nm) on the concentrations of **poly-PA-α-Glc**, **poly-PA-β-Glc**, **poly-PA-α-Gal**, and **poly-PA-β-Gal** in PBS (pH 7.4).

Lectin Recognition Properties of Glycoconjugated Poly(phenylacetylene)s. To provide preliminary insights into the lectin recognition properties of the poly(phenylacetylene)s with diversified saccharide functionalities, fluorescence quenching titrations were examined using fluorescein isothiocyanate labeled Concanavalin A (FITC-Con A) and peanut agglutinin (FITC-PNA). Con A and PNA are plant lectins consisting of four specific binding sites for the glucose and galactose units, respectively.^{16a} FITC groups have an intrinsic emission peak at 517 nm that is quenched upon binding to saccharides, making it possible to quantify the host–guest binding.¹⁷ As expected, the addition of the glycoconjugated poly(phenylacetylene)s resulted in the quenching of the FITC fluorescence (Figure 5A,B). Efficient binding to FITC-Con A was observed for the **poly-PA-α-Glc** and **poly-PA-β-Glc**; the values of the relative change in the fluorescence intensity ($\Delta F/F_0$) for **poly-PA-α-Glc** and **poly-PA-β-Glc** showed a nonlinear decrease as a function of the concentration of the Glc unit, whereas **poly-PA-α-Gal** and **poly-PA-β-Gal** showed slight decrease of the $\Delta F/F_0$ derived from the weak nonspecific binding of the Gal unit to Con A (Figure 5A). Likewise, **poly-PA-α-Gal** and **poly-PA-β-Gal** displayed prominent affinities for PNA, whereas **poly-PA-α-Glc** and **poly-PA-β-Glc** did not (Figure 5B). These results clearly suggest that the three-dimensional organized saccharide clusters along the polyacetylene backbones have strong binding affinities toward specific lectins depending on the saccharide functionalities.

To provide further insight into the “cluster glycoside effect”^{1e}, the association constants (K_a) of the poly(phenylacetylene)s carrying saccharide clusters to lectins were experimentally quantified by the Scatchard plot as follows:¹⁷

$$\frac{[\text{sugar}]F_0}{\Delta F} = \frac{[\text{sugar}]F_0}{\Delta F_{\text{max}}} + \frac{F_0}{\Delta F_{\text{max}}K_a}$$

where [sugar], F_0 , and F are the concentrations of the glycoconjugates, the initial fluorescence intensity of the FITC-lectins, and the fluorescence intensity, respectively. Figure 6A shows the Scatchard plots for the **poly-PA-α-Glc** and **poly-PA-β-Glc** binding to FITC-Con A. The K_a 's for these interactions were determined from the slopes and the intercepts of Figure 6A (Table 2). The highly clustered effect of **poly-PA-α-Glc** was observed due to the α-Glc units on the poly(phenylacetylene), resulting in enhancement of the specific binding with Con A; the K_a for **poly-PA-α-Glc** between Con A ($1.4 \times 10^5 \text{ M}^{-1}$) was about 82 times greater than that of methyl α-D-glucopyranoside ($1.7 \times 10^3 \text{ M}^{-1}$).^{16b} In addition, the prominent affinity of **poly-PA-β-Glc** for Con A ($K_a = 5.1 \times 10^4 \text{ M}^{-1}$) was half that for **poly-PA-α-Glc**, although β-glucosides generally have a much weaker affinity for Con A than the α-glucosides.^{16a,b} These results highlight the fact that the affinities of these glycoconjugates toward Con A were significantly affected by the three-dimensional saccharides organization.

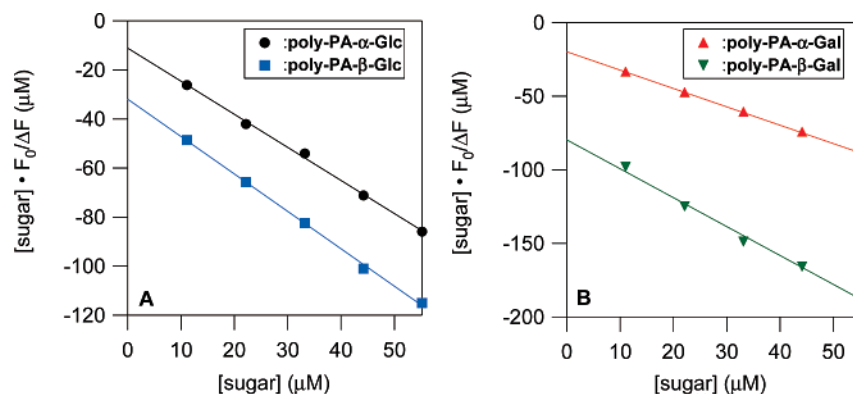


Figure 6. Scatchard plots of fluorescence intensity change in FITC-Con A with **poly-PA-α-Glc** and **poly-PA-β-Glc** (A) and FITC-PNA with **poly-PA-α-Gal** and **poly-PA-β-Gal** (B).

Table 2. K_a Values of Glycoconjugates to Con A and PNA

	K_a (M^{-1})	
	Con A	PNA
poly-PA-α-Glc	1.4×10^5	
poly-PA-β-Glc	5.1×10^4	
methyl α-D-glucopyranoside	1.7×10^3 ^a	
methyl β-D-glucopyranoside	7.0×10^4	
poly-PA-α-Gal		6.3×10^4
poly-PA-β-Gal		2.5×10^4
methyl α-D-galactopyranoside		1.8×10^3 ^b
methyl β-D-galactopyranoside		1.0×10^3 ^b

^a K_a of methyl α- and β-D-glucopyranoside was from the literature (see reference 16b). ^b K_a of methyl α- and β-D-galactopyranoside was from the literature (see reference 16c).

For PNA, the K_a values for **poly-PA-α-Gal** ($6.3 \times 10^4 M^{-1}$) and **poly-PA-β-Gal** ($2.5 \times 10^4 M^{-1}$) showed about 35 and 25-fold higher magnitudes for methyl α-D-galactopyranoside and methyl β-D-galactopyranoside, respectively (Table 2).^{16c} These results are again ascribed to the “cluster glycoside effect”. Comparison between **poly-PA-α-Gal** and **poly-PA-β-Gal** provides preliminary insights into the chiral spatial registration effects of the saccharides on the lectin recognition. Given that **poly-PA-α-Glc** and **poly-PA-β-Glc** have the same sense of helicity and **poly-PA-α-Gal** and **poly-PA-β-Gal** have the opposite helicity featuring the saccharide functionalities within the poly(phenylacetylene) backbones (Figure 4, vide supra), a significant difference in the binding efficiency was observed between **poly-PA-α-Gal** and **poly-PA-β-Gal**. There was essentially no difference in the recognition affinity of the α- and β-galactose units to PNA, supporting the importance of the three-dimensional saccharide arrangement in the lectin recognition of helical saccharide arrays.

Conclusions

In summary, we successfully synthesized poly(phenylacetylene)s bearing D-glucopyranose and D-galactopyranose with controlled anomeric configurations with predominantly one-handed helical conformations induced by the saccharide functionalities. The helical backbone conformations of these glycoconjugated polymers were drastically changed in response to the solvent accompanied by a visible color change. These glycoconjugates had strong affinities for specific lectins, such as Con A and PNA, responding to the specificity of the saccharide residue. In addition, the affinities of these glycoconjugates for the lectins were strongly affected by the backbone-chirality based on the one-handed helical conformations. The highly stereoregular saccharide arrays constructed on the chiral helical backbone should be responsible for this

affinity effect. Further research on the glycoconjugates bearing other kinds of saccharides with a controlled backbone conformation is now in progress.

Acknowledgment. This study was partly supported by a Grant-in-Aid for Japan Society for the Promotion of Science (JSPS) Fellows.

Supporting Information Available: The synthesis procedure and ¹H NMR spectrum of **poly(PA_{0.5}-co-PA-α-Glc-OAc_{0.5})**, the CD and UV-vis spectra of **poly-PA-β-Glc-OAc**, **poly-PA-α-Gal-OAc**, **poly-PA-β-Gal-OAc**, **poly-PA-α-Glc**, **poly-PA-β-Glc**, **poly-PA-α-Gal**, and **poly-PA-β-Gal**. This material is available free of charge via the Internet at <http://pubs.acs.org>.

References and Notes

- (a) Lee, Y. C.; Lee, R. T. *Acc. Chem. Res.* **1995**, *28*, 321–327. (b) Dwek, R. A. *Chem. Rev.* **1996**, *96*, 683–720. (c) Mammen, M.; Choi, S. K.; Whitesides, G. M. *Angew. Chem., Int. Ed.* **1998**, *37*, 2754–2794. (d) Lis, H.; Sharon, N. *Chem. Rev.* **1998**, *98*, 637–674. (e) Lundquist, J. J.; Toone, E. J. *Chem. Rev.* **2002**, *102*, 555–578. (f) De Pez, J. L.; Seeberger, P. H. *QSAR Comb. Sci.* **2006**, *11*, 1027–1032.
- Roy, R.; Zanini, D.; Meunier, S. J.; Romanowska, A. *J. Chem. Soc., Chem. Commun.* **1993**, 1869–1872.
- Aoi, K.; Itoh, K.; Okada, M. *Macromolecules* **1995**, *28*, 5391–5393.
- Ashton, P. R.; Boyd, S. E.; Brown, C. L.; Jayaraman, N.; Nepogodiev, S. A.; Stoddart, J. F. *Chem.—Eur. J.* **1996**, *2*, 1115–1128.
- (a) Imai, T.; Satoh, T.; Kaga, H.; Kaneko, N.; Kakuchi, T. *Macromolecules* **2003**, *36*, 6359–6363. (b) Satoh, T.; Imai, T.; Ishihara, H.; Maeda, T.; Kitajyo, Y.; Narumi, A.; Kaga, H.; Kaneko, N.; Kakuchi, T. *Macromolecules* **2003**, *36*, 6364–6370. (c) Imai, T.; Satoh, T.; Kaga, H.; Kaneko, N.; Kakuchi, T. *Macromolecules* **2004**, *37*, 3113–3119. (d) Imai, T.; Nawa, Y.; Kitajyo, Y.; Satoh, T.; Kaga, H.; Kaneko, N.; Kakuchi, T. *Macromolecules* **2005**, *38*, 1648–1654. (e) Satoh, T.; Imai, T.; Ishihara, H.; Maeda, T.; Kitajyo, Y.; Sakai, Y.; Kaga, H.; Kaneko, N.; Ishii, F.; Kakuchi, T. *Macromolecules* **2005**, *38*, 4202–4210. (f) Kitajyo, Y.; Imai, T.; Sakai, Y.; Tamaki, M.; Tani, H.; Takahashi, K.; Narumi, A.; Kaga, H.; Kaneko, N.; Satoh, T.; Kakuchi, T. *Polymer* **2007**, *48*, 1237–1244.
- (a) Kobayashi, K.; Sumitomo, H.; Ina, Y. *Polym. J.* **1985**, *17*, 567–575. (b) Kobayashi, K.; Sumitomo, H.; Itoigawa, T. *Macromolecules* **1987**, *20*, 906–908. (c) Kobayashi, K.; Tsuchida, A.; Usui, T.; Akaike, T. *Macromolecules* **1997**, *30*, 2016–2020.
- Kobayashi, K.; Kakishita, M.; Okada, M.; Akaike, T.; Usui, T. *J. Carbohydr. Chem.* **1994**, *13*, 753–766.
- Matsuura, K.; Furuno, S.; Kobayashi, K. *Chem. Lett.* **1998**, *27*, 847–848.
- Hasegawa, T.; Kondoh, S.; Matsuura, K.; Kobayashi, K. *Macromolecules* **1999**, *32*, 6595–6603.
- Kishimoto, Y.; Itou, M.; Miyatake, T.; Ikariya, T.; Noyori, R. *Macromolecules* **1995**, *28*, 6662–6666.
- Ma, D.-L.; Shum, T. Y.-T.; Zhang, F.; Che, C.-M.; Yang, M. *Chem. Commun.* **2005**, 4675–4677.
- Cheng, H.; Cao, X.; Xian, M.; Fang, L.; Cai, T. B.; Ji, J. J.; Tunac, J. B.; Sun, D.; Wang, P. G. *J. Med. Chem.* **2005**, *48*, 645–652.
- Yashima, E.; Huang, S.; Matsushima, T.; Okamoto, Y. *Macromolecules* **1995**, *28*, 4184–4193.

- (14) The synthesis procedure of **poly(PA_{0.5}-co-PA- α -Glc-OAc_{0.5})** was described in the supporting information.
- (15) Maeda, K.; Mochizuki, H.; Watanabe, M.; Yashima, E. *J. Am. Chem. Soc.* **2006**, *128*, 7639–7650.
- (16) (a) Sharon, N.; Lis, H. *Lectins*, 2nd ed.; Springer: The Netherlands, 2003. (b) Loontjens, F. G.; Van Wauwe, J. P.; De Bruyne, C. K. *Carbohydr. Res.* **1975**, *44*, 150–153. (c) Neurohr, K. J.; Young, N. M.; Mantsch, H. H. *J. Biol. Chem.* **1980**, *255*, 9205–9209. (d) Kaladas, P. M.; Kabat, E. A.; Iglesias, J. L.; Lis, H.; Sharon, N. *Arch. Biochem. Biophys.* **1982**, *217*, 624–637.
- (17) (a) Miura, Y.; Ikeda, T.; Kobayashi, K. *Biomacromolecules* **2003**, *4*, 410–415. (b) Miura, Y.; Wada, N.; Nishida, Y.; Mori, H.; Kobayashi, K. *J. Polym. Sci., Part A: Polym. Chem.* **2004**, *42*, 4598–4606.

MA7020776